Communication

Heat-Transfer Analysis of the Promotion of the CO_2 Reduction Performance of a P_4O_{10}/TiO_2 Photocatalyst Using a Black Body Material

Akira Nishimura [1],*, Ryo Hanyu [1], Homare Mae [1], Hiroki Senoue [1] and Eric Hu [2]

[1] Division of Mechanical Engineering, Graduate School of Engineering, Mie University, 1577 Kurimamachiya-cho, Tsu 514-8507, Mie, Japan; 423m139@m.mie-u.ac.jp (R.H.); 422m146@m.mie-u.ac.jp (H.M.); 420147@m.mie-u.ac.jp (H.S.)

[2] School of Electrical and Mechanical Engineering, The University of Adelaide, Adelaide 5005, Australia; eric.hu@adelaide.edu.au

* Correspondence: nisimura@mach.mie-u.ac.jp; Tel.: +81-59-231-9747

Abstract: Since photocatalytic reactions are surface reactions, enhancing gas movement around the photocatalyst could improve photocatalytic CO_2 reduction performance. A new approach using black body material to enhance the gas movement around the photocatalyst based on the natural thermosiphon movement of gases around a photocatalyst has been proposed and confirmed experimentally, but the heat-transfer mechanism of the phenomena has not yet been clarified. The aim of this study is to clarify the corresponding heat-transfer mechanism. This study calculated the temperature of the CO_2/NH_3 gas mixture around a P_4O_{10}/TiO_2 photocatalyst using the heat-transfer formula. No difference was found between the temperature increase (T_g) from the temperature at the beginning of the CO_2 reduction experiment (T_{ini}) and the temperature of the CO_2/NH_3 gas mixture measured experimentally via thermocouple (T_e) under the following illumination conditions: a Xe lamp with visible light (VIS) + infrared light (IR) and IR only. The heat-transfer model proposed in this study predicts T_g well under illumination from a Xe lamp with VIS + IR as well as under IR illumination only. On the other hand, the difference found between T_g and T_e was as large as 10 °C under illumination from a Xe lamp with ultraviolet light (UV) + VIS + IR.

Keywords: heat-transfer analysis; P_4O_{10}/TiO_2 photocatalyst; CO_2 reduction with NH_3; black body material; infrared light; mass-transfer promotion

1. Introduction

Photocatalysis is a promising technology for utilizing sunlight, i.e., renewable energy. The photocatalytic reduction process can convert CO_2 into fuel species such as CO, CH_4, CH_3OH, etc. [1–3]. TiO_2 is a popular photocatalyst used for CO_2 reduction. However, TiO_2 works only under UV light illumination, which accounts for only 4% of sunlight [4]. On the other hand, visible light (VIS) and infrared light (IR) account for 44% and 52% of the solar energy reaching the Earth's surface, respectively [4]. If a photocatalyst absorbing VIS and IR could be developed, the performance of CO_2 reduction could be improved significantly.

According to a literature review [1,5], many attempts have been made to extend the light absorption of a photocatalyst from ultraviolet light (UV) to VIS or near IR. Metal doping is normally used to extend the light absorption performance of a photocatalyst from UV to VIS [1]. Cu, Fe, Ag, Au and In, etc. have been investigated as dopants. Ag-nano particles/TiO_2 nanowire exhibited excellent performance, producing 983 μmol/g of CO [6,7], which is 109 times as much as pure TiO_2. Several photocatalyst studies have reported extending the absorption of light wavelengths up to IR [8–11]. Under illumination from light ranging in wavelength from 200 nm to 2400 nm, a $W_{18}O_{49}$/g-C_3N_4 composite produced 45 μmol/g of CO and 28 μmol/g of CH_4 [8]. A WS_2/Bi_2S_3 nanotube exhibited the

absorption of VIS and near IR light (wavelength: 420 nm–1100 nm), producing 28 μmol/g of CH_3OH and 25 μmol/g of C_2H_5OH [9]. CuInZnS-decorated g-C_3N_4 extended the range of absorbed wavelengths of light from 200 nm to 1000 nm, producing 38 μmol/g of CO [10]. Hierarchical $ZnIn_2S_4$ nanorods prepared using the solvothermal method produced 54 μmol/g of CO and 9 μmol/g of CH_4 [11].

In previous studies [12,13], the authors prepared P_4O_{10}/TiO_2, which successfully extended the absorbed wavelength of light up to IR. Under IR illumination, the largest molar quantity of CO per unit weight of photocatalyst for the P_4O_{10}/TiO_2 film in the case of CO_2/H_2O was 2.36 μmol/g, while that in the case of CO_2/NH_3 was 33.4 μmol/g [12,13].

Another way of promoting CO_2 reduction performance is to enhance gas movement around the photocatalyst, which was proposed by the authors [14,15], who found that the mass transfer time of 10^5 s to 10^{-1} s was longer than the photoreaction time of 10^{-9} s to 10^{-15} s [16]. Consequently, mass transfer was an inhibition issue for improving the CO_2 reduction performance of a photocatalyst. Another reason for the low reforming rate of photocatalytic CO_2 reduction was the reorganization of the products. Since the reaction surface of the photocatalyst was covered by products, the movement of the reactants to the reaction surface was inhibited, and the reverse reaction, i.e., reoxidation, which reproduces CO_2 from products such as CO and CH_4 was favored. Consequently, CO and CH_4 are hopefully removed from the reaction surface as soon as they are produced. On the other hand, the authors investigated a new approach using a black body material to enhance gas movement around a photocatalyst based on the natural thermosiphon movement of gases around a photocatalyst [14,15]. According to the literature survey conducted by the authors, no study other than the authors' previous studies [14,15] has used a black body material for the promotion of mass transfer and photocatalytic CO_2 reduction performance. Therefore, the concept of promoting mass transfer around the photocatalyst using a black body material for the improvement of photocatalytic CO_2 reduction performance, which is proposed in this study, is original to the authors. CO_2 reduction performance was improved through the use of a black body material with the appropriate heat capacity by enhancing the natural thermosiphon movement of gases around a TiO_2 photocatalyst [14]. The maximum concentration of CO formed using black body materials was two to five times as large as was the case using no black body material [14]. In addition, this effect was also confirmed for the case of a P_4O_{10}/TiO_2 photocatalyst absorbing VIS and IR [15]. Under illumination from a Xe lamp with IR only, the concentration of CO formed using a black body material compared to no black body material increased from 4 ppmV to 13 ppmV, and the temperature in the reactor rose from 2.0 °C to 3.1 °C. It can be claimed that the use of a black body material enhances mass transfer surrounding the photocatalyst via the natural thermosiphon movement of gases around the photocatalyst [14,15]. However, the heat-transfer mechanism of the phenomenon has not yet been clarified. Further promoting the CO_2 reduction performance of the photocatalyst requires revealing the heat-transfer mechanism underlying the temperature rise.

Consequently, the aim of this study is to reveal the heat-transfer mechanism underlying the rise in gas temperature around the photocatalyst after heat absorption by a black body material. This study calculates the temperature of the gases around the photocatalyst using heat-transfer formulas and compares this to the temperature of the gases measured via thermocouple in the CO_2 reduction experiment from the authors' previous study [15].

2. Results and Discussion

Heat-Transfer Mechanism for the Temperature Increase of the CO_2/NH_3 Gas Mixture Surrounding the P_4O_{10}/TiO_2 Photocatalyst Due to the Black Body Material

This study calculated the increase in the temperature of the CO_2/NH_3 gas mixture (T_g) from the initial temperature (T_{ini}) at the beginning of the CO_2 reduction experiment. Table 1 compares T_g values to the temperature of the CO_2/NH_3 gas mixture measured experimentally via thermocouple (T_e) in the authors' previous study [15]. The measurement accuracy of the thermocouple used in the authors' previous study [15] was 0.1 °C. In

addition, the temperatures, which were measured for 10 min using the thermocouple [15], were applied in this study. In this study, the illumination time of the Xe lamp for the photocatalytic CO_2 reduction experiment was 8 h, which was in keeping with the authors' previous studies [12–15]. According to the authors' previous work, the formation rate of CO attains its maximum value at approximately 2 h of Xe illumination and decreases gradually. The formation rate of CO after 8 h of Xe illumination is nearly 0. Therefore, this study adopted a Xe illumination time of 8 h. The following table shows T_{ini}, T_g, T_e, $T_e - T_g$ and the percentage of absolute error T_{error}, i.e., $(T_g - T_e)/(T_g - T_{ini}) \times 100$, at different molar ratios under Xe illumination with UV + VIS + IR, VIS + IR and IR only. This table indicates the effect of the temperature rise due to the black body material. Table 2 shows the relationship between the maximum concentration of CO formed and T_e in the reactor obtained from the authors' experimental study [15] (included here for the reader's understanding). The data with and without the black body material are shown in this table.

Table 1. Comparison of T_{ini} (initial temperature of the CO_2 reduction experiment), T_e (temperature of the CO_2/NH_3 gas mixture determined experimentally via thermocouple), T_g (temperature increase of the CO_2/NH_3 gas mixture), $T_e - T_g$ and T_{error} at different molar ratios under Xe illumination with UV + VIS + IR, VIS + IR and IR only.

			UV + VIS + IR			
CO_2 [mol]	NH_3 [mol]	T_{ini} [°C]	T_g [°C]	T_e [°C]	$T_e - T_g$ [°C]	T_{error} [%]
1	0.5	24.7	36.7	46.5	9.8	−44.7
1	1	24.0	36.5	44.9	8.4	−40.0
1	2	24.1	36.8	45.2	8.4	−39.9
1	4	24.2	36.9	45.2	8.3	−39.6
3	2	24.1	36.4	45.9	9.5	−43.6
3	8	24.4	37.1	45.2	8.1	−38.9
			VIS + IR			
CO_2 [mol]	NH_3 [mol]	T_{ini} [°C]	T_g [°C]	T_e [°C]	$T_e - T_g$ [°C]	T_{error} [%]
1	0.5	25.4	36.3	36.8	0.5	−4.47
1	1	25.0	36.3	36.7	0.4	−3.15
1	2	24.5	36.0	35.6	−0.4	3.36
1	4	24.6	36.1	35.4	−0.7	6.20
3	2	24.3	35.4	35.5	0.1	−0.731
3	8	24.4	35.9	34.2	−1.7	17.2
			IR only			
CO_2 [mol]	NH_3 [mol]	T_{ini} [°C]	T_g [°C]	T_e [°C]	$T_e - T_g$ [°C]	T_{error} [%]
1	0.5	25.3	34.2	34.8	0.6	−6.79
1	1	24.6	33.8	34.8	1.0	−9.67
1	2	24.6	33.9	34.9	1.0	−9.44
1	4	24.4	33.7	35.6	1.9	−16.7
3	2	24.7	33.7	35.0	1.3	−12.2
3	8	25.0	34.3	34.3	0	0.374

Table 1 shows that $T_e - T_g$ was nearly zero under Xe illumination with VIS + IR and IR only. Therefore, the heat-transfer model proposed in this study predicted T_g well under Xe illumination with VIS + IR and IR only. On the other hand, Table 1 shows that $T_e - T_g$ was larger under Xe illumination with UV + VIS + IR. We assume that the heat absorbed due to the black body material was converted from the source light. In the heat-transfer

analysis, the heat absorbed by the black body material was calculated using the light intensity measured using the light intensity meter. However, the heat converted from the light at each wavelength was not calculated exactly. The emissive power of black body is a function of the wavelength of light and increases with the increase in the wavelength of light, especially within the IR range [16]. Therefore, the heat absorbed by the black body material under Xe illumination with UV + VIS + IR might be underestimated in this study.

Table 2. Relationship between the maximum concentration of the CO formed and the T_e obtained from the authors' experimental study [15].

UV + VIS + IR (without black body material)			
CO$_2$ [mol]	NH$_3$ [mol]	T_e [°C]	The maximum concentration of CO formed [ppmV]
1	0.5	16.8	318
1	1	16.8	353
1	2	15.6	342
1	4	15.2	362
3	2	18.3	410
3	8	15.1	291
UV + VIS + IR (with black body material)			
CO$_2$ [mol]	NH$_3$ [mol]	T_e [°C]	The maximum concentration of CO formed [ppmV]
1	0.5	21.8	340
1	1	20.9	401
1	2	21.1	413
1	4	21.0	404
3	2	21.8	461
3	8	20.8	370
VIS + IR (without black body material)			
CO$_2$ [mol]	NH$_3$ [mol]	T_e [°C]	The maximum concentration of CO formed [ppmV]
1	0.5	7.8	124
1	1	7.5	153
1	2	7.7	154
1	4	7.1	147
3	2	7.9	205
3	8	8.1	141
VIS + IR (with black body material)			
CO$_2$ [mol]	NH$_3$ [mol]	T_e [°C]	The maximum concentration of CO formed [ppmV]
1	0.5	11.1	153
1	1	11.7	181
1	2	11.1	194
1	4	10.8	176
3	2	12.0	224
3	8	9.8	169

Table 2. *Cont.*

IR only (without black body material)			
CO_2 [mol]	NH_3 [mol]	T_e [°C]	The maximum concentration of CO formed [ppmV]
1	0.5	7.3	39
1	1	7.6	45
1	2	8.1	47
1	4	7.5	45
3	2	8.1	53
3	8	7.0	42
IR only (with black body material)			
CO_2 [mol]	NH_3 [mol]	T_e [°C]	The maximum concentration of CO formed [ppmV]
1	0.5	9.1	48
1	1	10.2	56
1	2	10.2	58
1	4	10.2	50
3	2	10.3	66
3	8	9.3	46

Table 3 lists the T_g and $T_e - T_g$ values calculated using the heat absorbed by the black body materials—which were 1.6 to 1.7 times larger than those given for T_g in Table 1—at different molar ratios under Xe illumination with UV + VIS + IR. Table 3 shows that $T_e - T_g$ values for the heat absorbed by the black body material were 1.6 times larger than those given for T_g in Table 1 and ranged from 0.5 °C to 2.5 °C. In addition, $T_e - T_g$ values for the heat absorbed by the black body material were 1.7 times larger than those given for T_g in Table 1 and ranged from −0.8 °C to 1.3 °C. Table 3 reveals that $T_e - T_g$ values decreased compared to those shown in Table 1, indicating that the prediction accuracy of the heat model proposed in this study could be improved. Therefore, the authors would like to investigate the procedure for measuring light intensity according to the lighting conditions and the heat conversion process for each wavelength of light in the near future.

This study confirms that black body materials enhance mass transfer around the P_4O_{10}/TiO_2 photocatalyst via the natural thermosiphon movement of gases around the P_4O_{10}/TiO_2 photocatalyst. The photocatalytic reaction occurs on the surface of the P_4O_{10}/TiO_2 photocatalyst. Since the photocatalytic CO_2 reduction product covers the surface of the P_4O_{10}/TiO_2 photocatalyst, the new reductants, i.e., CO_2 and NH_3, cannot reach the surface of the P_4O_{10}/TiO_2 photocatalyst. This decreases photocatalytic CO_2 reduction performance. Using black body material, which can absorb the light, causes the product remaining around the P_4O_{10}/TiO_2 photocatalyst to be heated and to lighten. After that, the product moves upward, stirring the gas around the P_4O_{10}/TiO_2 photocatalyst. Then, the new reductants, i.e., CO_2 and NH_3, can reach the surface of the P_4O_{10}/TiO_2 photocatalyst, thereby improving photocatalytic CO_2 reduction performance. Since the photocatalytic reaction is a surface reaction, we can claim that this approach effectively improves mass transfer. Figure 1 illustrates the concept of the mechanism for mass transfer around the photocatalyst, which is promoted by the natural thermosiphon gas movement created around the photocatalyst by the black body materials in this study.

Table 3. Comparison of values for T_{g}, $T_{\mathrm{e}} - T_{\mathrm{g}}$ and T_{error}, which were calculated using the heat absorbed by the black body materials at different molar ratios under Xe illumination with UV + VIS + IR; these values were 1.6 to 1.7 times larger than those given for T_{g} in Table 1.

1.6 Q				
CO_2 [mol]	NH_3 [mol]	T_{g} [°C]	$T_{\mathrm{e}} - T_{\mathrm{g}}$ [°C]	T_{error} [%]
1	0.5	44.0	2.5	−11.6
1	1	44.1	0.8	−4.04
1	2	44.4	0.8	−3.76
1	4	44.5	0.7	−3.33
3	2	43.8	2.1	−9.73
3	8	44.7	0.5	−2.31
1.7 Q				
CO_2 [mol]	NH_3 [mol]	T_{g} [°C]	$T_{\mathrm{e}} - T_{\mathrm{g}}$ [°C]	T_{error} [%]
1	0.5	45.2	1.3	−6.05
1	1	45.3	−0.4	2.00
1	2	45.7	−0.5	2.25
1	4	45.8	−0.6	2.71
3	2	45.0	0.9	−4.10
3	8	46.0	−0.8	3.80
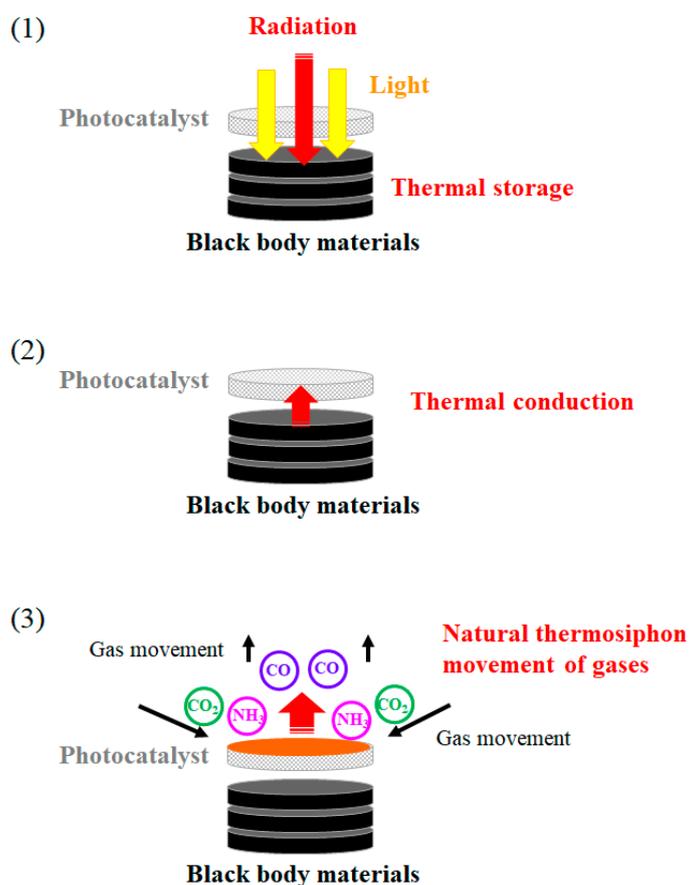
Figure 1. Concept of the mechanism for mass transfer around the photocatalyst, which is promoted by the natural thermosiphon gas movement created around the photocatalyst by black body material (Phenomenon order: (1) → (2) → (3)).

According to the concept of this study, to improve photocatalytic CO_2 reduction performance, it is important to balance the temperature of the gases in the reactor, photocatalyst, black body material, reactor surface and air surrounding the reactor. In addition, it is important to record experimental data for the temperature and the concentration of the CO formed under the various light conditions in order to clarify the prediction accuracy of the model. The experimental setup adopted in this study and its size limitations make it difficult to record these data [15]. The authors would therefore like to redesign the experimental setup for a CO_2 reduction experiment in the near future.

3. Calculation Procedure for Heat-transfer Analysis

Heat-Transfer Formulas

This study considered the heat transfer from a P_4O_{10}/TiO_2 photocatalyst that was coated onto a net-like glass disc fitted on the black body materials to the gases over the P_4O_{10}/TiO_2 photocatalyst. This study assumed that the source light is ultimately converted to heat and absorbed by the black body materials. Since the light intensity differed depending on the light conditions, the converted heat that was absorbed by the black body materials decreased in the following order: UV + VIS + IR, VIS + IR, IR only. The temperature of the CO_2/NH_3 gas mixture, T_g, was calculated using the following formula:

$$Q = hA(T_g - T_{ini}) \tag{1}$$

where Q is the heat absorbed by the black body materials [Q], h is the heat-transfer coefficient [$W/(m^2 \cdot K)$], A is the heat-transfer area (=the surface area of the Cu disc on one side) [m^2], T_{ini} is the initial temperature of the CO_2 reduction experiment) [15] [K]. This study assumed that T_g is equal to the surface temperature of the P_4O_{10}/TiO_2 photocatalyst and the black body material. In other words, this study assumed that the CO_2/NH_3 gas mixture was heated from T_{ini} to T_g via the P_4O_{10}/TiO_2 photocatalyst and the black body material. h was calculated using the following formula:

$$h = \frac{Nu \cdot \lambda}{d} \tag{2}$$

where Nu is the Nusselt number [-], λ is the thermal conductivity of the CO_2/NH_3 gas mixture [$W/(m \cdot K)$] and d is the representative length for each local Nu [m]. Nu was obtained from the following formula, which can be applied to laminar-free convection heat transfer over a vertical flat plate [17]:

$$Nu_x = \frac{0.631 Pr^{\frac{2}{5}}}{\left(Pr + 0.9\sqrt{Pr} + 0.4\right)^{\frac{1}{5}}} \left(\frac{g\beta q x^4}{\nu^2 \lambda}\right)^{\frac{1}{5}} \tag{3}$$

where Pr is the Prandtl number [-], g is the gravitational acceleration (=9.81) [m^2/s], β is the volume expansion coefficient [$1/K$], q is the heat-transfer rate (=Q/A), x is the position (=5 mm intervals up to the Cu disc radius of 25 mm) [m] and ν is the kinetic viscosity [m^2/s]. The physical properties are calculated at the mean temperature of a quartz glass installed under the Xe lamp, which is 343 K, and the maximum temperature of the CO_2/NH_3 gas mixture measured via thermocouple in the CO_2 reduction experiment [15]. Under these conditions, the Pr values for CO_2 and NH_3 were 0.766 and 0.95, respectively [17]. The ν values for CO_2 and NH_3 were 0.0097×10^{-6} m^2/s and 0.51525×10^{-6} m^2/s, respectively [18]. The λ values for CO_2 and NH_3 were 19.94×10^{-3} $W/(m \cdot K)$ and 42.95×10^{-3} $W/(m \cdot K)$, respectively [17]. The β values for CO_2 and NH_3 were 3.722×10^{-6} $1/K$ and 3.790×10^{-6} $1/K$, respectively. Each physical property was calculated for the different CO_2/NH_3 molar ratios based on the weight ratio of the CO_2/NH_3 gas mixture. This study assumed that Q is ultimately converted from the source light and was calculated using the light intensity measured under each set of

illumination conditions, i.e., 1.08 W for UV + VIS + IR, 0.952 W for VIS + IR and 0.735 W for IR only. A was 1963×10^{-6} m^2.

Using the equations shown above, T_g was obtained for each molar ratio of CO_2/NH_3 under each set of illumination conditions. In addition, T_g was compared to the maximum temperature measured via thermocouple in the CO_2 reduction experiment in the authors' previous study [15].

4. Conclusions

This study developed a simple convective heat-transfer model to calculate the temperature of the CO_2/NH_3 gas mixture around the P_4O_{10}/TiO_2 photocatalyst and the black body material in the reactor, which was validated by experimental data in the authors' previous study [15]. As a result, the following conclusions were drawn:

(i) The heat-transfer model proposed in this study was found to predict T_g well under Xe illumination with VIS + IR and IR only.

(ii) $T_e - T_g$ was found to be higher, i.e., 10 °C higher, under Xe illumination with UV + VIS + IR relative to Xe illumination with VIS + IR and IR only.

(iii) $T_e - T_g$ under the Xe illumination with UV + VIS + IR decreased upon increasing the heat absorbed by black body materials; these values were 1.6 to 1.7 times larger than those calculated using the light intensity measured with the light intensity meter.

(iv) According to the heat-transfer analysis conducted in this study, mass transfer around the P_4O_{10}/TiO_2 photocatalyst was promoted by the natural thermosiphon movement of the gases, which was generated around the P_4O_{10}/TiO_2 photocatalyst by the black body material.

Author Contributions: Conceptualization and writing—original draft preparation, A.N.; data curation and formal analysis, R.H.; methodology, H.M. and H.S.; writing—review and editing, E.H. All authors have read and agreed to the published version of the manuscript.

Conflicts of Interest: The authors declare no conflict of interest.

References

1. Jesic, D.; Jurkovic, L.D.; Pohar, A.; Suhadolnik, L.; Likozar, B. Engineering Photocatalytic and Photoelectrocatalytic CO$_2$ Reduction Reactions: Mechanisms, Intrinsic Kinetics, Mass Transfer Resistances, Reactors and Multi-scale Modeling Simulations. *Chem. Eng. J.* **2021**, *407*, 126799. [CrossRef]
2. Kaushik, R.; Singh, P.K.; Halder, A. Modulation Strategies in Titania Photocatalyst for Energy Recovery and Environmental Remediation. *Catal. Today* **2022**, *384–386*, 45–69. [CrossRef]
3. Wang, Z.W.; Shi, Y.Z.; Liu, C.; Kang, Y.Y.; Wu, L. Cu$^+$-Ti^{3+} Interface Interaction Mediated CO$_2$ Coordination model for Controlling the Selectivity of Photocatalytic Reduction CO$_2$. *Appl. Catal. B Environ.* **2022**, *301*, 120803. [CrossRef]
4. Remiro-Buenamanana, S.; Garcia, H. Photoassisted CO$_2$ Conversion into Fuels. *Chem. Cat Chem. Minirev.* **2019**, *11*, 342–356. [CrossRef]
5. Cai, Y.; Luo, F.; Guo, Y.; Guo, F.; Shi, W.; Yang, S. Near-Infrared Light Driven ZnIn$_2$S$_4$-Based Photocatalysts for Environmental and Energy Applications: Progress and Perspectives. *Molecules* **2023**, *28*, 2142. [CrossRef] [PubMed]
6. Tahir, M. Synergistic Effect in MMT-Dispersed Au/TiO$_2$ Monolithic Nanocatalyst for Plasma-Absorption and Metallic Interband Transitions Dynamic CO$_2$ Photoreduction to CO. *Appl. Catal. B Environ.* **2017**, *219*, 329–343. [CrossRef]
7. Tahir, M.; Tahir, B.; Amin, N.A.S. Synergistic Effect in Plasmonic Au/Ag Alloy NPs Co-Coated TiO$_2$ NWs toward Visible-Light Enhanced CO$_2$ Photoreduction to Fuels. *Appl. Catal. B Enviorn.* **2017**, *204*, 548–560. [CrossRef]
8. Hong, L.F.; Guo, R.T.; Yuan, Y.; Ji, X.Y.; Lin, Z.D.; Gu, J.W.; Pan, W.G. Urchinlike W$_{18}$O$_{49}$/g-C$_3$N$_4$ Z-Scheme Heterojunction for Highly Efficient Photocatalytic Reduction of CO$_2$ under Full Spectrum Light. *Energy Fuels* **2021**, *35*, 11468–11478. [CrossRef]
9. Dai, W.; Yu, J.; Luo, S.; Hu, X.; Yang, L.; Zhang, S.; Li, B.; Luo, X.; Zou, J. WS$_2$ Quantum Dots Seeding in Bi$_2$S$_3$ Nanotubes: A Novel Vis-NIR Light Sensitive Photocatalyst with Low-Resistance Junction Interface for CO$_2$ Reduction. *Chem. Eng. J.* **2020**, *389*, 123430. [CrossRef]
10. Gan, J.; Wang, H.; Hu, H.; Su, M.; Chen, F.; Xu, H. Efficient Synthesis of Tunable Band-Gap CuInZnS Decorated g-C$_3$N$_4$ Hybrids for Enhanced CO$_2$ Photocatalytic Reduction and Near-Infrared-Triggered Photordegradation Performance. *Appl. Surf. Sci.* **2021**, *564*, 150396. [CrossRef]

11. Yu, M.; Lv, X.; Idris, A.M.; Li, S.; Lin, J.; Lin, H.; Wang, J.; Li, Z. Upconversion Nanoparticles Coupled with Hierarchical ZnIn$_2$S$_4$ Nanorods as a Near-Infrared Responsive Photocatalyst for Photocatalytic CO$_2$ Reduction. *J. Colloid Interface Sci.* **2022**, *612*, 782–791. [CrossRef] [PubMed]

12. Nishimura, A.; Mae, H.; Kato, T.; Hu, E. Utilization from ultraviolet to infrared light for CO$_2$ reduction with P$_4$O$_{10}$/TiO$_2$ photocatalyst. *Phys. Astron. Int. J.* **2022**, *6*, 145–154. [CrossRef]

13. Nishimura, A.; Mae, H.; Hannyu, R.; Hu, E. Impact of loading amount of P$_4$O$_{10}$ on CO$_2$ reduction performance of P$_4$O$_{10}$/TiO$_2$ with H$_2$O extending absorption range from ultraviolet to infrared light. *Phys. Astron. Int. J.* **2022**, *6*, 186–194. [CrossRef]

14. Nishimura, A.; Kato, T.; Mae, H.; Hu, E. Impact of black body material enhanced gas movement on CO$_2$ photocatalytic reduction performance. *Catalysts* **2022**, *12*, 470. [CrossRef]

15. Nishimura, A.; Hanyu, R.; Mae, H.; Hu, E. Impact of Black Body Material on CO$_2$ Reduction Performance of P$_4$O$_{10}$/TiO$_2$ with NH$_3$. *J. Phys. Chem. Res.* **2023**, *5*. [CrossRef]

16. Holman, J.P. *Heat Transfer*, 8th ed.; McGRAW-HILL, INC.: New York, NY, USA, 1997; p. 400.

17. Aihara, T. *Heat Transfer Engineering*, 1st ed.; Syokabo: Tokyo, Japan, 1994; pp. 107, 274.

18. Hasatani, M.; Kimura, J. *Basis and Application for Combustion*, 2nd ed.; Kyoritsu Shuppan: Tokyo, Japan, 1986; p. 276.